The Voronoi Diagram of Circles and Its Application to the Visualization of the Growth of Particles

François Anton[1], Darka Mioc[2], and Christopher Gold[3]

[1] Department of Informatics and Mathematical Modelling
Technical University of Denmark
Richard Petersens Plads
DK-2800 Kongens Lyngby
Denmark
fa@imm.dtu.dk
[2] Department of Geodesy and Geomatics Engineering
University of New Brunswick
P.O. Box 4400
Fredericton, New Brunswick, Canada, E3B 5A3
dmioc@unb.ca
[3] School of Computing
University of Glamorgan
Pontypridd, CF37 1DL, UK
cmgold@glam.ac.uk

Abstract. Circles are frequently used for modelling the growth of particle aggregates through the Johnson-Mehl tessellation, that is a special instance of the Voronoi diagram of circles. Voronoi diagrams allow one to answer proximity queries after locating a query point in the Voronoi zone it belongs to. The dual graph of the Voronoi diagram is called the Delaunay graph. In this paper, we first show a necessary and sufficient condition of connectivity of the Voronoi diagram of circles. Then, we show how the Delaunay graph of circles (the dual graph of the Voronoi diagram of circles) can be computed exactly, and in a much simpler way, by computing the eigenvalues of a two by two matrix. Finally, we present how the Voronoi diagram of circles can be used to model the growth of particle aggregates. We use the Poisson point process in the Voronoi diagram of circles to generate the Johnson-Mehl tesselation. The Johnson-Mehl model is a Poisson Voronoi growth model, in which nuclei are generated asynchronously using a Poisson point process, and grow at the same radial speed. Growth models produce spatial patterns as a result of simple growth processes and their visualization is important in many technical processes.

Keywords: Voronoi diagram of circles, Visualization of nucleation and growth of particles, Johnson-Mehl tessellations, growth models.

1 Introduction

The proximity queries among circles could be effectively answered if the Delaunay graph for sets of circles could be computed in an efficient and exact way.

M.L. Gavrilova and C.J.K. Tan (Eds.): Trans. on Comput. Sci. III, LNCS 5300, pp. 20–54, 2009.

This would require the embedding of the Delaunay graph and the location of the query point in that embedded graph. The embedded Delaunay graph and the Voronoi diagram are dual subdivisions of space, which can be stored in a quad-edge data structure [GS85]. The original contribution of this paper is a necessary and sufficient condition of connectivity of the Voronoi diagram of circles, an exact and much simpler algorithm for the Delaunay graph of circles (the dual graph of the Voronoi diagram of circles, with no assumption on the disjointness of circle sites), and its application to the visualization of the growth of particles.

The first and most explored Voronoi diagram is the Voronoi diagram for a set of points [Vor07, Vor08, Vor10] in the Euclidean plane or in the three-dimensional Euclidean space (see Figure 1). Voronoi diagrams have been generalised in many different ways including by modifying the space in which they are embedded (see [Auren87, OBSC01] for a general survey of Voronoi diagrams): higher dimensional Euclidean spaces, non Euclidean geometries (e.g. Laguerre geometry, hyperbolic geometry, etc.). Fewer generalisations of Voronoi diagrams correspond to extending the possible sites from points to circles, i.e., the additively weighted Voronoi diagram (see Figure 2) [AMG98b, AMG98a] and the Voronoi diagram for circles (set of sites comprising circles, see Figure 3) [KKS01b, KKS01a, KKS00]. The definition of the weighted Voronoi diagram differs from the definition of the ordinary one in that the Euclidean distance is replaced by a weighted distance. In the case of the additively weighted Voronoi diagram, the weighted distance between a point and a generator is the Euclidean distance minus the weight of the generator, but since it must be a distance, it has to be always positive or zero, and thus the additively weighted distance is not defined in the interior of the weight circles (circles centred on a generator and of radius the weight of the generator). The additively weighted Voronoi diagram has been extensively studied by Ash and Bolker [AB86] and Aurenhammer [Auren88] under the name of hyperbolic Dirichlet tessellations and Power Voronoi diagrams, but till [AMG98b] and [AMG98a], there was no dynamic algorithm for constructing the additively weighted Voronoi diagram. This work solves the robustness issue in the work of Anton, Mioc and Gold [AMG98b, AMG98a] and extends it to the Voronoi diagram of circles. This robustness fix and extension are achieved by providing an exact conflict locator.

The exact computation of the additively weighted Voronoi diagram has not been addressed until Anton et al. [ABMY02]. That paper addressed the exact predicate for the off-line construction of the dual graph of the additively weighted Voronoi diagram from the dual of the Power Voronoi diagram of spheres by using the relationship between the additively weighted Voronoi diagram in the plane and the Power Voronoi diagram[1] of spheres in the three-dimensional space. In their independent work, Karavelas and Emiris [KE02, EK06, KE03] provided several exact predicates of maximum degree 16 for achieving the same "in-circle/orientation/edge-conflict-type/difference of radii" test as we do in a single

[1] The Power Voronoi diagram is a generalised Voronoi diagram where sites are hyperspheres and the distance between a point and a site is the power of that point with respect to that site [Auren87].

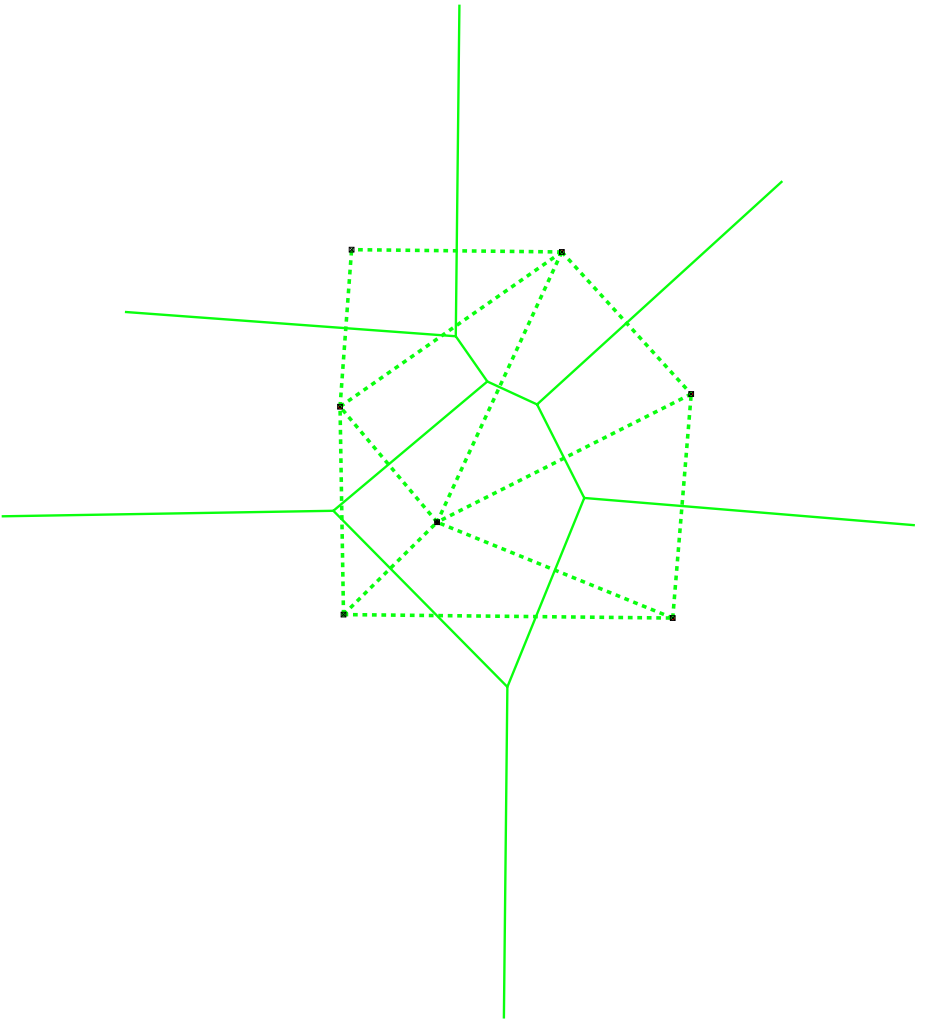

Fig. 1. The ordinary Voronoi diagram (plain lines) of points (squares), and its topology expressed by the Delaunay triangulation (dashed lines)

conflict locator presented in this paper. They reduced the degree of their predicate from 28 to 20 and then to 16 using Sturm sequences and invariants. Their work is more limited in scope than ours, because they compute the additively weighted Voronoi diagram (or Appolonius diagram) rather than the Voronoi diagram of circles, and they assume the circles never intersect (they mention this assumption could be lifted, but they provide no justification), and they also assume no three circles can have a common tangent, or equivalently, no empty circle has infinite radius. The difference between the additively weighted Voronoi diagram (or Appolonius diagram) and the Voronoi diagram of circles is that the additively weighted Voronoi diagram (or Appolonius diagram) is based

on a distance that is not defined in the interior of the (weight) circles, while the Voronoi diagram of circles is based on a distance that is defined everywhere. Thus, there can not be a point of the additively weighted Voronoi diagram in the interior of a circle, because its distance to the enclosing circle is not defined. Thus intersecting circles are not permitted and circles contained in other circles are not permitted either. Indeed, a point of the Voronoi diagram in the interior of the enclosing circle would not have a defined distance to the enclosing circle. The approach adopted in [KE02, EK06, KE03] is also more complex than ours, because they compute exactly not only the Delaunay graph, but also the additively weighted Voronoi diagram, which unlike they state, is not required in the applications. Only the exact computation of the Delaunay graph of circles is required for practical applications, because the Delaunay graph gives the topology of circles. Finally, our approach is much simpler, because we obtain the output of the predicate (in fact a Delaunay graph conflict loctor) by computing the sign of the eigenvalues of a simple two by two matrix.

In this paper, we also provide an application of the Voronoi diagram of circles to the visualisation of the growth of particle aggregates, which justifies the motivation for not only computing the additively weighted Voronoi (or Appolonius) diagram, but also the Voronoi diagram of circles. A comprehensive overview of the Delaunay and Voronoi methods for non-crystalline structures was provided by Medvedev [Med00], and Anishchik and Medvedev [AM95] were the first ones in 1995 to provide the solution of Appolonius problem for sphere packing in three dimensions. The application of the additively weighted Voronoi diagram to visualization of the growth of particle aggregates is based on particle statistics. Particle statistics play an important role in many technical processes (in the industrial production of materials where the phase transition from liquid to solid is a part of the technical process, for example production of metals and ceramic materials) [Stoya98], material science, plant ecology, and spatial analysis. Due to the lack of efficient algorithms for their visualization only the "set-theoretic approach in particle statistics" [Stoya98] has been used as a method of visualization of spatial growth processes in the past.

Growth models produce spatial patterns as a result of simple growth processes operating with respect to a set of n points (nucleation sites), $\mathcal{P} = \{p_1, p_2, ...p_n\}$ at positions $x_1, x_2, ..., x_n$, respectively in $\mathbb{R}^m$ or a bounded region of $\mathbb{R}^m$ $(m = 2, 3)$. The growth processes such as agglomeration, aggregation, packing, etc. lead in a natural way to the Poisson Voronoi tessellation [OBSC01], [Stoya98] and to the Johnson-Mehl tessellation when the members of the generator set $\mathcal{P}$ are not contemporaneous [OBSC01].

The Johnson-Mehl model has been introduced in [JM39] for modelling the growth of particle aggregates. The Johnson-Mehl model is a Poisson Voronoi growth model, in which nuclei are generated asynchronously using a Poisson point process [OBSC01], and grow at the same radial speed v. Each generator $P_i = (\overrightarrow{p_i}, t_i)$ has both a planar location (its position vector) and an associated birth time t_i $(t_i \geq 0)$. The Johnson-Mehl tessellation can be considered as a generalisation of a dynamic version of an additively weighted Voronoi diagram

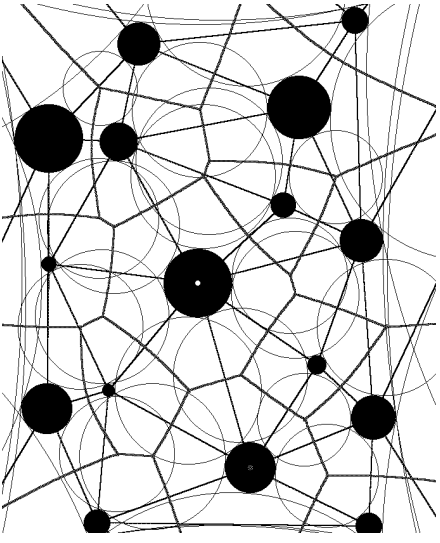

Fig. 2. An additively weighted Voronoi diagram, its dual graph and the empty circumcircles

[AMG98a], in which the weight reflects the arrival time of the point in $\mathbb{R}^2$ [OBSC01]. However, since when nuclei start to touch as they grow, the Johnson-Mehl tessellation might have intersecting nuclei, and edges that correspong to loci of centres of circles internally tangent to two weight circles. In that case, the additively weighted distance would not be well defined, because it would be negative. In that case, the distance used is the distance corresponding to the Voronoi diagram of circles. Thus, the Johnson-Mehl tessellation differs from the Voronoi diagram of circles in that only bisectors that are loci of circles that are either externally tangent to 2 circles or internally tangent to 2 circles are boundaries of Johnson-Mehl cells.

This paper is organised as follows. In Section 2, we present the definitions of the (generalised) Voronoi diagram of a set of sites and its dual Delaunay graph of a set of sites, and the Delaunay graph conflict locator. In Section 3, we provide necessary and sufficient conditions for construction of the Delaunay graph of circles and for connectivity of the Voronoi diagram of circles. In Section 4, we present the Delaunay graph conflict locator, both in the case of the additively weighted Voronoi diagram, and the Voronoi diagram of circles. In Section 5, we present the application of the Voronoi diagram to the modelling and the visualisation of the growth of particle aggregates. Finally, we present the conclusions and future work in Section 6.

2 Preliminaries

Voronoi diagrams are irregular tessellations of the space, where space is continuous and structured by discrete objects [AK00, OBSC01]. The Voronoi diagram

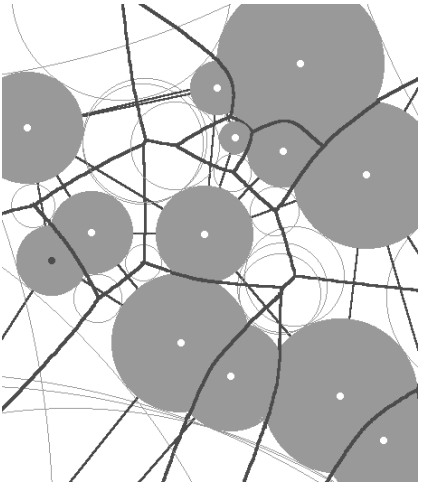

Fig. 3. The Voronoi diagram, the Delaunay graph and the empty circumcircles of circles. The circles hide the edges of the Delaunay graph between intersecting circles and the empty circles corresponding to intersecting circles.

[Vor07, Vor08, Vor10] (see Figure 1) of a set of sites is a decomposition of the space into proximal regions (one for each site). Sites were points for the first historical Voronoi diagrams [Vor07, Vor08, Vor10], but in this paper we will explore sets of circles. The proximal region corresponding to one site (i.e. its Voronoi region) is the set of points of the space that are closer to that site than to any other site of the set of sites [OBSC01]. We will recall now the formal definitions of the Voronoi diagram and of the Delaunay graph. For this purpose, we need to recall some basic definitions.

Definition 1. (Metric) Let M be an arbitrary set. A *metric* on M is a mapping $d : M \times M \rightarrow \mathbb{R}_+$ such that for any elements a, b, and c of M, the following conditions are fulfilled: $d(a,b) = 0 \Leftrightarrow a = b$, $d(a,b) = d(b,a)$, and $d(a,c) \leq d(a,b) + d(b,c)$. (M,d) is then called a *metric space*, and $d(a,b)$ is the distance between a and b.

Remark 2. The Euclidean space $\mathbb{R}^N$ with the Euclidean distance δ is a metric space $\left(\mathbb{R}^N, \delta\right)$.

Let $M = \mathbb{R}^N$, and δ denote a distance between points. Let $\mathcal{S} = \{s_1, ..., s_m\} \subset M, m \geq 2$ be a set of m different subsets of M, which we call *sites*. The distance between a point x and a site $s_i \subset M$ is defined as $d(x, s_i) = \inf_{y \in s_i} \{\delta(x,y)\}$.

Definition 3. (Bisector) For $s_i, s_j \in \mathcal{S}, s_i \neq s_j$, the *bisector* $B(s_i, s_j)$ of s_i with respect to s_j is: $B(s_i, s_j) = \{x \in M | d(x, s_i) = d(x, s_j)\}$ (see Figure 4).

Definition 4. (Influence zone) For $s_i, s_j \in \mathcal{S}, s_i \neq s_j$, the *influence zone* $D(s_i, s_j)$ of s_i with respect to s_j is: $D(s_i, s_j) = \{x \in M | d(x, s_i) < d(x, s_j)\}$ (see Figure 5).

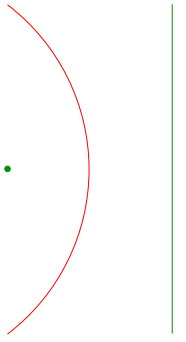

Fig. 4. The bisector (parabola) of a point and a line segment

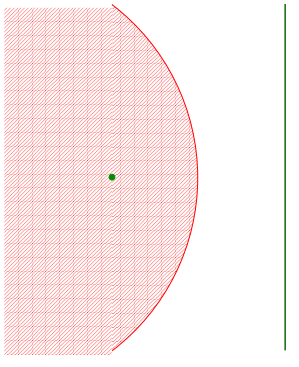

Fig. 5. The influence zone (hashed) of a point with respect to a line

Definition 5. (Voronoi region) The *Voronoi region* $V(s_i, \mathcal{S})$ of $s_i \in \mathcal{S}$ with respect to the set $\mathcal{S}$ is: $V(s_i, \mathcal{S}) = \bigcap_{s_j \in \mathcal{S}, s_j \neq s_i} D(s_i, s_j)$.

Definition 6. (Voronoi diagram) The *Voronoi diagram* of $\mathcal{S}$ is the union $V(\mathcal{S}) = \bigcup_{s_i \in \mathcal{S}} \partial V(s_i, \mathcal{S})$ of all region boundaries (see example on Figure 3).

Definition 7. (Delaunay graph) The *Delaunay graph* $DG(\mathcal{S})$ of $\mathcal{S}$ is the dual graph of $V(\mathcal{S})$ defined as follows:

- the set of vertices of $DG(\mathcal{S})$ is $\mathcal{S}$,
- for each $(N-1)-$dimensional facet of $V(\mathcal{S})$ that belongs to the common boundary of $V(s_i, \mathcal{S})$ and of $V(s_j, \mathcal{S})$ with $s_i, s_j \in \mathcal{S}$ and $s_i \neq s_j$, there is an edge of $DG(\mathcal{S})$ between s_i and s_j and reciprocally, and
- for each vertex of $V(\mathcal{S})$ that belongs to the common boundary of $V(s_{i_1}, \mathcal{S})$,..., $V\left(s_{i_{N+2}}, \mathcal{S}\right)$, with $\forall k \in \{1, ..., N+2\}, s_{i_k} \in \mathcal{S}$ all distinct, there exists a complete graph K_{N+2} between the s_{i_k}, and reciprocally (see example on Figure 3).

The one-dimensional elements of the Voronoi diagram are called Voronoi edges. The points of intersection of the Voronoi edges are called Voronoi vertices. The Voronoi vertices are points that have at least $N + 1$ nearest neighbours among the sites of $\mathcal{S}$. In the plane, the Voronoi diagram forms a network of vertices and edges. In the plane, when sites are points in general position, the Delaunay graph is a triangulation known as the Delaunay triangulation. In the plane, the Delaunay graph satisfies the following empty circle criterion: no site intersects the interior of the circles touching (tangent to without intersecting the interior of) the sites that are the vertices of any triangle of the Delaunay graph.

Once the Voronoi region a query point belongs to has been identified, it is easy to answer proximity queries. The closest site from the query point is the site whose Voronoi region is the Voronoi region that has been identified. The Voronoi diagram defines a neighbourhood relationship among sites: two sites are neighbours if, and only if, their Voronoi regions are adjacent, or alternatively, there exists an edge between them in the Delaunay graph.

The exact computation of the Delaunay graph is important for two reasons. By exact computation, we mean a computation whose output is correct. First, unlike the Voronoi diagram, the Delaunay graph is a discrete structure, and thus it does not lend itself to approximations. Second, the inaccurate computation of this Delaunay graph can induce inconsistencies within this graph (see Section 4.2), which may cause a program that updates this graph to crash. This is particularly true for the randomised incremental algorithm for the construction of the Voronoi diagram of circles. In order to maintain the Delaunay graph after each addition of a site, we need to detect the Delaunay triangles that are not empty any longer, and we need to detect which new triangles formed with the new site are empty, and thus valid. In the reminder, sites are generators of the Voronoi diagram or the Delaunay graph, while points are any location in the plane unless specified otherwise. The algorithm that certifies whether the triangle of the Delaunay graph whose vertices are 3 given sites is empty (i.e. does not contain any point of a given site in its interior) or not empty is used for checking which old triangles are not empty any longer and which new triangles formed with the new site are empty, and thus valid. This algorithm is called the "*Delaunay graph conflict locator*" in the reminder of this paper.

When the old triangles are checked, its input is a 4-tuple of sites, where the first three sites define an old triangle, and the fourth site is the new site being inserted. When the new triangles are checked, its input is also a 4-tuple of sites, where the first three sites define a new triangle, the first two sites being linked by an existing Delaunay edge, and the fourth site forms an old Delaunay triangle with the first two sites. Its output is the list of all the Voronoi vertices corresponding to the $1-$dimensional facets of the Delaunay graph having the first 3 sites as vertices whose circumcircles contain a point of the fourth site in their interior, and a value that certifies the presence of each Voronoi vertex in that list. The fact that a circumcircle (the circle that is externally tangent to three given circles) is not empty is equivalent to the triangle formed by those three circles being not Delaunay, and this is called a conflict. Thus, it justifies

the name of "Delaunay graph conflict locator". In the context of the ordinary Voronoi diagram of points in the plane, the concept that is analogous to the Delaunay graph conflict locator is the *Delaunay graph predicate*, which certifies whether a triangle of the Delaunay triangulation is such that its circumcircle does not contain a given point.

The exact knowledge of the Delaunay graph for curved objects may sound like a purely theoretical knowledge that is not central in practical applications. This is not always the case in some applications. These applications include material science, metallography, spatial analyses and VLSI layout. The Johnson-Mehl tessellations (which generalise several weighted Voronoi diagrams) [OBSC01] play a central role in the Kolmogorov-Johnson-Mehl-Avrami [JM39, Kol37] nucleation and growth kinetics theory. The Kolmogorov theory provides an exact description of the kinetics during the heating and cooling processes in material science (the Kolmogorov equation [JM39, Kol37]). The exact knowledge of the neighbourliness among molecules is central to the prediction of the formation of particle aggregates. In metallography, the analysis of precipitate sizes in aluminium alloys through Transmission Electronic Microscopy [Des03, Section 1.2.2] provides an exact measurement of the cross sections of these precipitates when they are "rodes" with a fixed number of orientations [Des03, Section 1.2.2]. In VLSI design, the second order Voronoi diagram of the layout is used in the computation of the critical area, a measure of a circuit layout's sensitivity to spot defects [CPX02, Section 1]. An important concern on critical area computation is robustness [CPX02, Section 1].

Another limitation of approximative algorithms for the computation of the Delaunay graph is that when approximate computations are performed on objects defined approximately (within some geometric tolerance), the propagation of the errors can be critical, especially if the final computation involves approximate intermediary computations.

Finally, the exact computation of the Delaunay graph participates to the recent move in the development of numerical and simulation software as well as computer algebra systems to exact systems [BCSS98].

3 The Necessary and Sufficient Conditions of Construction of the Delaunay Graph of Circles and of Connectivity of the Voronoi Diagram of Circles

In this section, we will examine how the Delaunay graph conflict locator can be used to maintain the Voronoi diagram of circles in the plane as those circles are introduced one by one. Finally, we will give a necessary and sufficient condition for the connectivity of the Voronoi diagram of circles in the projective plane that has a direct application in the representation of spatial data at different resolutions.

Knowing the Voronoi diagram $V(\mathcal{S})$ of a set $\mathcal{S}=\{s_1, \ldots, s_m\} \subset \mathbb{R}^2$ of at least two circles ($m > 1$) and its embedded Delaunay graph $DG(\mathcal{S})$ stored in a quad-edge data structure, we would like to get the Voronoi diagram $V(\mathcal{S} \cup \{s_{m+1}\})$,

where s_{m+1} is a circle of $\mathbb{R}^2$. In all this section, we will say that a circle $\mathcal{C}$ *touches* a circle s_i if, and only if, $\mathcal{C}$ is tangent to s_i and no point of s_i is contained in the interior of $\mathcal{C}$.

The Voronoi edges and vertices of $V(\mathcal{S})$ may or may not be present in $V(\mathcal{S} \cup \{s_{m+1}\})$. Each new Voronoi vertex w induced by the addition of s_{m+1} necessarily belongs to two Voronoi edges of $V(\mathcal{S})$, because two of the three closest sites to w necessarily belong to $\mathcal{S}$. The new Voronoi edges induced by the addition of s_{m+1} will clearly connect Voronoi vertices of $V(\mathcal{S})$ to new Voronoi vertices induced by the addition of s_{m+1} or new Voronoi vertices between themselves.

Any of these later Voronoi edges e' must be incident to one of the former Voronoi edges at each extremity of e' (because the Voronoi vertex at each extremity of e' belongs to only one new Voronoi edge, i.e. e'). Any of the former Voronoi edges e must be a subset of a Voronoi edge of $V(\mathcal{S})$, since e must be a new Voronoi edge between sites of $\mathcal{S}$ (otherwise the Voronoi vertex belonging to $V(\mathcal{S})$ at one of the extremities of e by the definition of e would be a new Voronoi vertex). Thus, to get $V(\mathcal{S} \cup \{s_{m+1}\})$, we need to know which Voronoi vertices and edges of $V(\mathcal{S})$ will not be present in $V(\mathcal{S} \cup \{s_{m+1}\})$, which Voronoi edges of $V(\mathcal{S})$ will be shortened in $V(\mathcal{S} \cup \{s_{m+1}\})$ and which new Voronoi edges will connect new Voronoi vertices between themselves.

We can test whether each Voronoi vertex v of $V(\mathcal{S})$ will be present in $V(\mathcal{S} \cup \{s_{m+1}\})$. Let us suppose that v is a Voronoi vertex of s_i, s_j and s_k. v will remain in $V(\mathcal{S} \cup \{s_{m+1}\})$ if, and only if, no point of s_{m+1} is contained in the interior of the circle centred on v that touches s_i, s_j and s_k. This is a sub-problem of the Delaunay graph conflict locator that can be tested by giving s_i, s_j, s_k and s_{m+1} as input to the Delaunay graph conflict locator, and then retain only the solutions where the Voronoi vertex is v.

We can test whether each Voronoi edge e of $V(\mathcal{S})$ will be present in $V(\mathcal{S} \cup \{s_{m+1}\})$. Let us suppose that e is a locus of points having s_i and s_j as closest sites. e will disappear entirely from $V(\mathcal{S} \cup \{s_{m+1}\})$ if, and only if, a point of s_{m+1} is contained in the interior of each circle centred on e and touching s_i, s_j and each common neighbour s_k to s_i and s_j in $DG(\mathcal{S})$ in turn. This can be tested by giving s_i, s_j, s_k and s_{m+1} as input to the Delaunay graph conflict locator and then retaining only the solutions where the Voronoi vertex belongs to e. e will be shortened (possibly inducing one or more new Voronoi edges) in $V(\mathcal{S} \cup \{s_{m+1}\})$ if, and only if, there exists Voronoi vertices of s_i, s_j and s_{m+1} on e and there is no point of any common neighbour s_k to s_i and s_j in $DG(\mathcal{S})$ in the interior of a circle centred on e and touching s_i, s_j and s_{m+1}. The centre of each one of such circles will be a new Voronoi vertex in $V(\mathcal{S} \cup \{s_{m+1}\})$. This can be tested by giving s_i, s_j, s_{m+1} and s_k as input to the Delaunay graph conflict locator and then retaining only the solutions where the Voronoi vertex belongs to e.

The Delaunay graph conflict locator is sufficient to maintain the Voronoi diagram of circles. Tests might be limited to edges and vertices on the boundaries of the Voronoi regions $V(s_i, \mathcal{S}), s_i \in \mathcal{S}$ that intersect s_{m+1} and of the Voronoi

regions $V(s_j, \mathcal{S}), s_j \in \mathcal{S}$ adjacent to a Voronoi region $V(s_i, \mathcal{S})$. Indeed, a point (and thus a circle) can steal its Voronoi region only from the Voronoi region it belongs to and the adjacent Voronoi regions.

We will finish this section with a necessary and sufficient condition for the connectivity of the Voronoi diagram of connected circles in the projective plane. This result allows the characterisation of dangling edges in the Delaunay graph corresponding to the presence of closed edges in the Voronoi diagram. In order to proceed, let us recall some notations used in point set topology: let $\overline{s}$ denote the closure of s, and $\overset{\circ}{s}$ denote the interior of s in the sense of the point set topology in $\mathbb{R}^2$. Note that if s bounds a closed domain then the interior of s is meant to be the interior of the closed domain bounded by s.

Proposition 8. *(Connectivity of the Voronoi diagram in the plane) The Voronoi diagram $V(\mathcal{S})$ of a set $\mathcal{S} = \{s_1, \ldots, s_m\} \subset \mathbb{R}^2$ of at least two connected circles ($m > 1$) considered in $\mathbb{P}^2$ is not connected if, and only if, there exist a subset I of $[1, \ldots, m]$ and one index j of $[1, \ldots, m]$ such that $\forall i \in I, s_i \subset \overset{\circ}{s_j}$ and $\forall k \in [1, \ldots, m] \setminus I, \overline{s_i} \cap \overline{s_k} = \overline{s_j} \cap \overline{s_k} = \emptyset$.*

Proof. If: Assume there exist a subset I of $[1, \ldots, m]$ and one index j of $[1, \ldots, m]$ such that $\forall i \in I, s_i \subset \overset{\circ}{s_j}$ and $\forall k \in [1, \ldots, m] \setminus I, \overline{s_i} \cap \overline{s_k} = \overline{s_j} \cap \overline{s_k} = \emptyset$. Let $s_l \in \mathcal{S}$ with $l \in [1, \ldots, m] \setminus I$. Let $S = \bigcup_{i \in I} s_i$. Since $S \subset \overset{\circ}{s_j}$, any circle touching both a $s_i, i \in I$ and s_j must be contained in $\overline{s_j}$. Since $\overline{S} \cap \overline{s_l} = \overline{s_j} \cap \overline{s_l} = \emptyset$, no circle can touch each of an $s_i, i \in I$, s_j and s_l. Thus, there is no point that has a $s_i, i \in I$, s_j and s_l as nearest neighbours. Thus, there is no Voronoi vertex of a $s_i, i \in I$, s_j and s_l. Since there is no Voronoi vertex of a $s_i, i \in I$, s_j and an s_l with $l \in [1, \ldots, m] \setminus I$, there are no Voronoi vertices on the bisector of S and s_j. Since $\overline{S} \cap \overline{s_l} = \overline{S} \cap \overline{s_l} = \emptyset$, any circle centred on the bisector of S and s_j and touching both S and s_j does not intersect any site s_k with $k \in [1, \ldots, m] \setminus I$. Thus, the bisector of S and s_j is contained in $V(\mathcal{S})$. Since s_j is connected and $S \subset \overset{\circ}{s_j}$, the bisector of S and s_j is a closed curve. Thus, the Voronoi diagram of $\mathcal{S}$ is not connected in $\mathbb{P}^2$.

Only if: Assume the Voronoi diagram of $\mathcal{S}$ is not connected in $\mathbb{P}^2$. Then, $V(\mathcal{S})$ has at least two connected components. Thus, at least one of these connected components does not have points at infinity. Let us consider the connected component (let us call it C_1) that does not have points at infinity. Since C_1 is composed of Voronoi edges[2], each edge in C_1 must end at either a Voronoi vertex or a point at infinity. Since C_1 does not have any point at infinity, all Voronoi edges in C_1 connect Voronoi vertices. Thus C_1 is a network of vertices and edges linking those vertices. The regions that this network defines are Voronoi regions. Let $\mathcal{D}$ be the union of the closure of those Voronoi regions. $\mathcal{D}$ is a closed set by its definition. Let us consider now the circles $s_l, l \in L$ whose Voronoi regions are contained in $\mathcal{D}$. Let $S = \bigcup_{l \in L} s_l$. Thus S is a union of circles.

[2] A one-dimensional component of the Voronoi diagram, which is also the locus of points having two nearest sites.

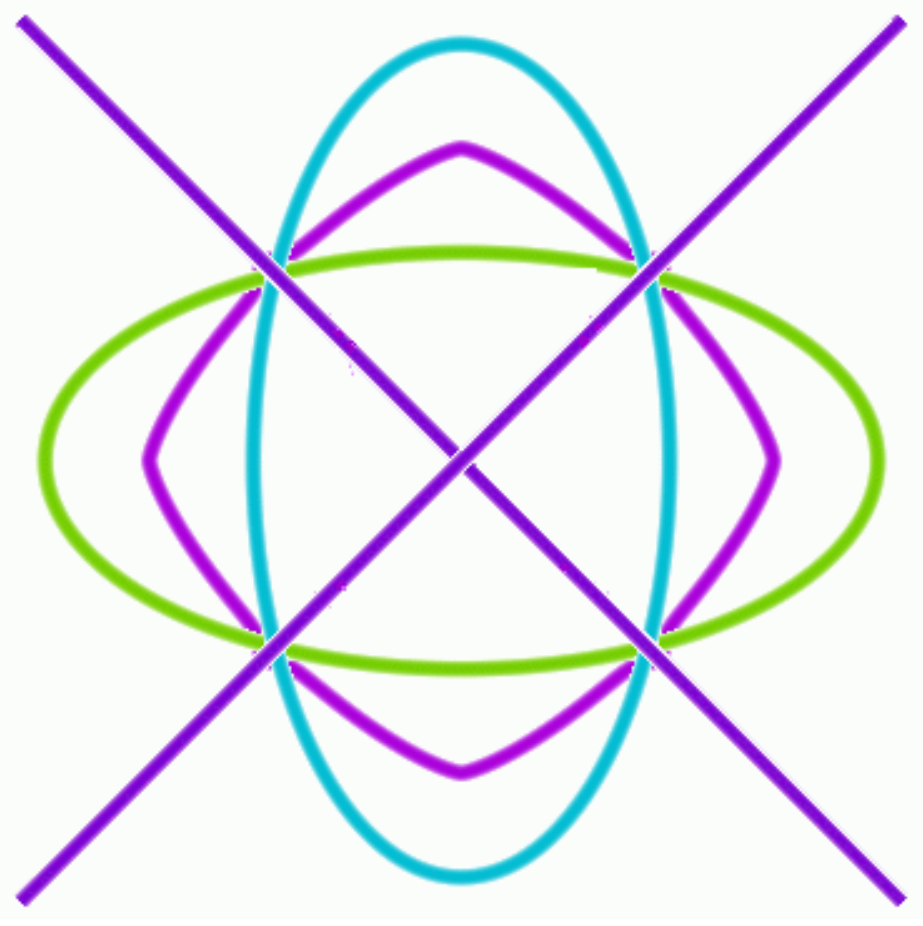

Fig. 6. The relative position with respect to the bisector must be constant

We will now consider S as a site instead of each one of the $s_l, l \in L$. The influence zone of $S = \bigcup_{l \in L} s_l$ is clearly $\mathring{\mathcal{D}}$, because the influence zone of a union of circles is clearly the closure of the union of the Voronoi regions of those circles. Let $e = \partial\mathcal{D}$. It is a portion of the bisector of S and another circle. Let us call it s_j. If not all the bisector of S and s_j was contained in $V(\mathcal{S})$, then e would end at Voronoi vertices (a point on the Voronoi diagram has at least two closest sites) or the point at infinity, a contradiction with e not being connected. Thus, the bisector of S and of s_j is contained in $V(\mathcal{S})$, and it is equal to e. By the definition of e, e must be a closed curve. Assume the positions of S and s_j with respect to e are not always the same. Then, S and s_j must intersect. The bisector of S and s_j must have two branches near the intersection points (see Figure 6). Since e is a closed curve and S is contained in the interior of e, s_j must be closed, and the other branches must be unbounded (a contradiction with e not being connected in $\mathbb{P}^2$). Thus, the positions of S and s_j with respect to e are always

the same along e. Since s_j is connected, S is contained in the interior of e and the positions of S and s_j with respect to e are always the same along e, $S \subset \overset{\circ}{s_j}$. Since e is the bisector of S and s_j and belongs to $V(\mathcal{S})$, any circle centred on e and touching both S and s_j does not intersect any site s_k with $k \in [1, \ldots, m] \setminus I$. Thus, $\forall k \in [1, \ldots, m] \setminus I, \overline{s_i} \cap \overline{s_k} = \overline{s_j} \cap \overline{s_k} = \emptyset$.

□

The only cases of disconnected (considered in $\mathbb{P}^2$) Voronoi diagrams correspond to one or more sites (circles) contained in the interior of another site. This property has a direct application in Geographic Information Systems. When the same region $\mathcal{R}$ bounded by a circle S is represented at different scales, the representation of the details inside $\mathcal{R}$ does not change the Voronoi diagram outside $\mathcal{R}$. The edges of the Delaunay graph corresponding to a disconnected Voronoi diagram (considered in $\mathbb{P}^2$) are respectively dangling edges or cut edges (the Delaunay graph is not bi-connected and removing a cut edge induces two connected components). It is possible to detect if there exists one or more sites $s_i, i \in I$ contained in the interior of another site s_j by checking that there exists no Voronoi vertex of s_i, s_j and any $s_k \in \mathcal{S}$ distinct from s_i and s_j. This is again a subproblem of the Delaunay graph conflict locator.

4 The Exact Symbolic Delaunay Graph Conflict Locator for Circles

We will first present the exact symbolic Delaunay graph conflict locator for additively weighted points when weighted points are introduced one by one, and then introduce what changes for circles. For this purpose, we will present some preliminaries about additively weighted Voronoi diagrams.

4.1 Preliminaries

Let $\mathbb{N}$ be the set of integers, $\mathbb{R}$ be the set of real numbers, and $\mathbb{R}^2$ be the Euclidean plane. Let $\mathcal{P} = \{P_1, ..., P_N\}$ be the set of generators or sites, where P_i is the *weighted point* located at $p_i \in \mathbb{R}^2$ and of weight $w_i \in \mathbb{R}$. Let C_i be the circle centred at p_i and of radius w_i, which we call *weight circle* hereafter.

The definitions of bisector, influence zone, Voronoi region and Voronoi diagram presented in Section 2 generalise to the case where the set of sites $\mathcal{S}$ is a set of weighted points $\mathcal{P}$, and the distance $d(M, P_i)$ (called *additive distance*) between a point M and a site P_i is $d(M, P_i) = \delta(M, p_i) - w_i$, where δ is the Euclidean distance between points.

The Voronoi region of P_i with respect to the set $\mathcal{P}$ is defined by: $\mathcal{V}(P_i, \mathcal{P}) = \left\{M \in \mathbb{R}^2 | \forall j \neq i : \delta(M, p_i) - w_i < \delta(M, p_j) - w_j\right\}$.

The *Additively Weighted Voronoi diagram* of $\mathcal{P}$ is defined by:

$V(\mathcal{P}) = \bigcup_{P_i \in \mathcal{P}} \partial V(P_i, \mathcal{P})$. The additively weighted Voronoi diagram is illustrated in Figure 7: the weight circles are drawn as plain disks with small holes at their centres, the additively weighted Voronoi diagram is drawn in plain thick hyperbola segments, and the Delaunay graph is drawn in dashed lines.

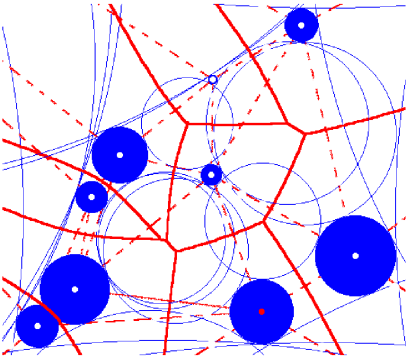

Fig. 7. The additively weighted Voronoi diagram

The additively weighted Voronoi diagram defines a network composed of edges (loci of points having two nearest neighbours), and vertices (loci of points having three nearest neighbours).

The additively weighted Voronoi diagram is related to the Apollonius Tenth problem. The Apollonius Tenth problem is to find a circle Γ tangent to three given circles C_1, C_2, C_3 (see Figure 8). For additively weighted points, we will see later in this section that only the circles that are either externally tangent to each of three given circles C_1, C_2, C_3 or internally tangent to each of C_1, C_2, C_3, are relevant to the Delaunay graph conflict locator. The centres of the circles that are solutions to the Apollonius Tenth problem are the first example encountered in this paper of generalised Voronoi vertices (a concept that we introduced in [Anton04]). Informally, generalised Voronoi vertices are the centres of circles tangent to $N + 1$ sites, where N is the dimension of the Euclidean space.

Hereafter we will call the solutions of the Apollonius Tenth problem *Apollonius circles*. The centres of the Apollonius circles that are either externally tangent to each of three given circles C_1, C_2, C_3 or internally tangent to each of C_1, C_2, C_3 are the first example encountered in this paper of true Voronoi vertices (i.e. centres of circles that touch $N + 1$ sites where N is the dimension of the Euclidean space).

4.2 The Delaunay Graph Conflict Locator for Additively Weighted Points

In this subsection, we present an exact algebraic conflict locator for the Delaunay graph of additively weighted points (i.e. the dual graph of the additively weighted Voronoi diagram). The maximum degree of the polynomials which need to be evaluated to compute this Delaunay conflict locator is 16 (thus, we say that the degree of the conflict locator is 16). This Delaunay graph conflict locator would be the core of a randomised incremental algorithm for constructing the additively weighted Voronoi diagram since the additively weighted Voronoi diagram is an abstract Voronoi diagram [Kle89], and thus, it can be constructed with the randomised incremental algorithm of Klein [Kle89].

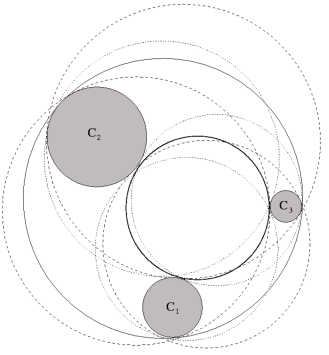

Fig. 8. The Apollonius Tenth problem

The motivation for an exact conflict locator lies in the fact that without an exact computation of the Delaunay graph of additively weighted points, some geometric and topologic inconsistencies may appear. This is illustrated with an example. The starting configuration is shown on Figure 9. There are three weighted points (whose corresponding weight circles are drawn). The Delaunay graph is drawn in dashed lines. The Apollonius circles tangent to the weight circles have been drawn in dotted lines. The real configuration after addition of a fourth weighted point is shown on Figure 10. The configuration that might have been computed by an approximate algorithm is shown on Figure 11: the difference between real and perceived situations has been exaggerated to show the difference. The old Apollonius circles have been adequately perceived to be invalid with respect to the newly inserted weighted point. About the new Voronoi vertices, while on the right of the figure two new Voronoi vertices have been identified as valid with respect to their potential neighbours, on the left of the figure, only one Voronoi vertex has been identified as being valid with respect to its potential neighbours. While the new Voronoi edge between the middle and bottom weighted points can be drawn between the two new Voronoi vertices of the new, middle and bottom weighted points; the Voronoi edge between the top and new weighted points cannot be drawn, because there is no valid Voronoi vertex on the left. There is an inconsistency within the topology: there is one new Voronoi vertex (the Voronoi vertex of the top new and middle weighted points) that cannot be linked by a new Voronoi edge to any other new Voronoi vertex and thus, that Voronoi vertex is incident to only two Voronoi edges. This additively weighted Voronoi diagram might have been computed by an approximative algorithm that is not an additively weighted Voronoi diagram. Thus, even if we perturbate the input weighted points, we will never get this additively weighted Voronoi diagram.

We consider the maintenance of the Delaunay graph of additively weighted points in an incremental way: we check the validity of all the triangles of the Delaunay graph whose vertices are P_1, P_2, P_3 with respect to a newly inserted weighted point P_4 [AKM02] or the validity of all the triangles of the Delaunay graph whose vertices are P_1, P_2, where the edge between P_1 and P_2 exists in

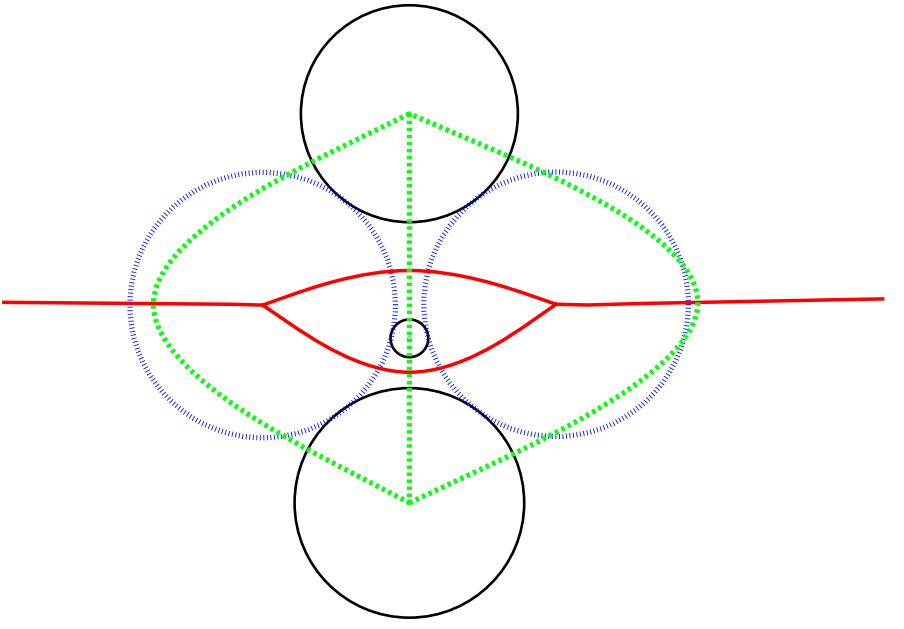

Fig. 9. The starting configuration

the Delaunay graph, and the newly inserted weight point P_3 with respect to an existing point P_4. Thus, the input of the conflict locator is constituted by four points: the first three are supposed to define a triangle in the Delaunay graph, and the last one is the tested point. Let (x_i, y_i) be the coordinates of p_i, for $i = 1, 2, 3, 4$. There are two possible outcomes to the above test of validity: either the triangles are valid with respect to the fourth weighted point and the triangles must appear in the Delaunay graph, or one or two triangles are not valid with respect to the fourth weighted point and those triangles will not be present in the Delaunay graph. We can see an example of the later case in Figure 12. A triangle having $P_1P_2P_3$ as vertices is not valid with respect to the weighted point P_4, because the circle externally tangent to both the weight circles C_1, C_2 and C_3 (of weighted points C_1, C_2 and C_3) contains a point of the weight circle C_4 (of the weighted point P_4). Thus, it must not appear in the Delaunay graph.

When the old triangles are checked, the conflict locator consists of determining which of the additively weighted Voronoi vertices of P_1, P_2 and P_3 will not remain after the insertion of P_4. When the new triangles are checked, the conflict locator consists of determining which new Voronoi vertices of weighted points P_1, P_2 and the newly inserted weighted point P_3 will appear, where P_1P_2 is an old Delaunay edge. When the new triangles are checked, this conflict locator tests the new triangle $P_1P_2P_4$ with respect to any point P_4 such that $P_1P_2P_4$ is an old Delaunay triangle. In both cases, the Delaunay graph conflict locator is equivalent in turn to the additive distance from which of the additively weighted Voronoi vertices of P_1, P_2 and P_3 to P_4 is smaller than the additive distance of that Voronoi vertex to P_1 (or P_2 or P_3 (see Figure 12).

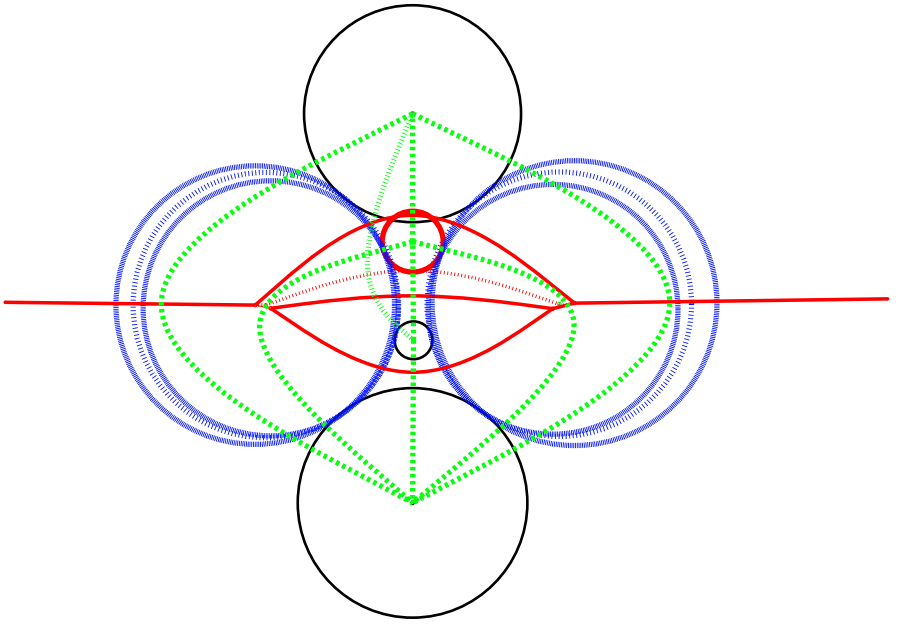

Fig. 10. The real configuration after addition of the fourth weighted point (bold weight circle)

Any *additively weighted Voronoi vertex* I of P_1, P_2, and P_3 with coordinates (x, y) can be obtained algebraically by computing the common intersection of the three circles C_1', C_2' and C_3' expanding (see Figure 13), or shrinking (see Figure 14) from the three first circles C_1, C_2 and C_3 all at the same rate. The common signed expansion of the first three circles is denoted by r. Each circle C'' centred on (x, y) and of radius r is either externally tangent to the first three circles (if the expansion r is positive) or internally tangent to the first three circles (if the expansion r is negative).

The centres coordinates x, y and radii r of the circles C'' centred on the intersections $I = C_1' \cap C_2' \cap C_3'$ and either externally or internally tangent to each of C_1, C_2, and C_3 can be computed algebraically as the solutions of the following system of three quadratic equations in the variables x, y and r:

$$\begin{cases} c_1'(x,y,r) = (x-x_1)^2 + (y-y_1)^2 - (w_1+r)^2 = 0 \\ c_2'(x,y,r) = (x-x_2)^2 + (y-y_2)^2 - (w_2+r)^2 = 0 \\ c_3'(x,y,r) = (x-x_3)^2 + (y-y_3)^2 - (w_3+r)^2 = 0 \end{cases}$$

Subtracting one of the equations (say $c_1'(x,y,r) = 0$) from the remaining two ($c_2'(x,y,r) = 0$ and $c_3'(x,y,r) = 0$) results in a system of 2 linear equations, from which x and y may be expressed as linear functions of r. Substitution in the first equation $c_1'(x,y,r) = 0$ then leads to a quadratic equation in r. This means that the unknown quantities x, y, r can be expressed with quadratic radicals as functions of the given centres and radii.

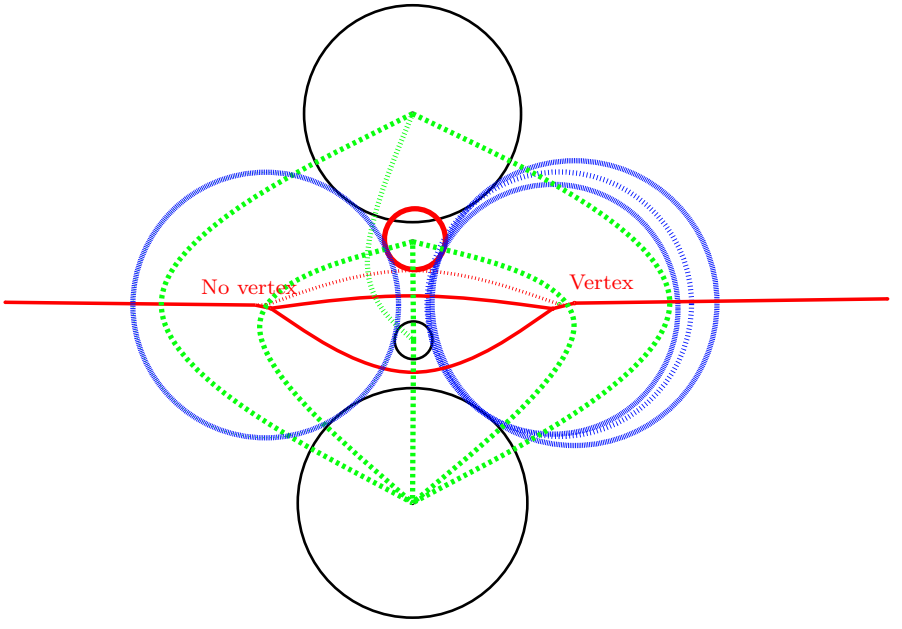

Fig. 11. The configuration computed by an approximate algorithm

Though the simplest thing to do now would be to compute the two Voronoi vertices and use their computed coordinates and corresponding signed expansion in the computation of the values certifying the output of the Delaunay graph conflict locator, it is not desirable because this method would not guarantee the topology of the Voronoi diagram of circles, nor its generalisation to conics or higher degree algebraic curves. We will detail hereafter only the computation of the values certifying the presence of Voronoi vertices in the output list.

To get the exact Delaunay graph conflict locator in a more elegant and generalisable way, we evaluated the values certifying the conflict locator output without relying on the computation of the Voronoi vertices as an intermediary computation. This is done by evaluating the values taken by the polynomial function expressing the relative position of C_4 with respect to C'' on the set of solutions of the system (i.e. the common zeroes of the three polynomials c'_1, c'_2 and c'_3). This is possible due to the translation that exists between geometry and algebra.

More specifically, to the geometric set X of the set of common zeroes of the three polynomials c'_1, c'_2 and c'_3 in K^3, where K is an algebraically closed field [Lan02, Definition before Theorem 1, Section 2, Chapter VII], we can associate the set of all polynomials vanishing on the points of X, i.e., the set of polynomials $f_1c'_1 + f_2c'_2 + f_3c'_3$ where the $f_i, i = 1, 2, 3$ are polynomials in the three variables x, y, r with coefficients in K. This set is the *ideal* [GP02, Definition 1.3.1] $\langle c'_1, c'_2, c'_3\rangle$. The set of polynomials with coefficients in K, forms with the addition and the multiplication of polynomials, a ring: the *ring of polynomials* [GP02, Definition 1.1.3]. A polynomial function $g\,(x, y, r)$ on K^3 is mapped to

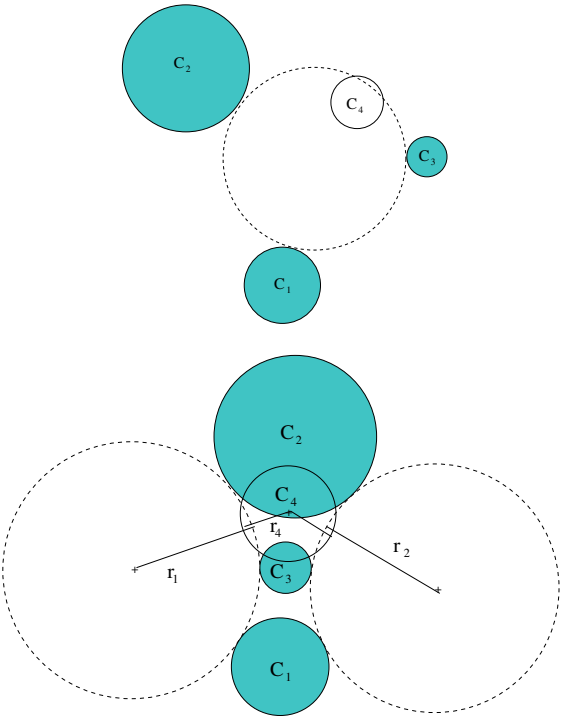

Fig. 12. The Delaunay graph conflict locator for the additively weighted Voronoi diagram: only the weight circles C_i or the weighted points P_i for $i = 1, ..., 4$ are shown. Up: there is only one Voronoi vertex to check; down: there are two Voronoi vertices to check.

a polynomial function on X if we recursively subtract from g any polynomial in g belonging to $\langle c'_1, c'_2, c'_3 \rangle$ until no monomial in g can be divided by each one of the lexicographically highest monomials in c'_1, c'_2 and c'_3. The result of this mapping gives a canonic representative of the remainder of the Euclidean division of the polynomial g by the polynomials c'_1, c'_2 and c'_3. The image of the ring of polynomials by this mapping is called the *quotient algebra* [Lan02, Section 3, Chapter II] of the ring of polynomials by the ideal $\langle c'_1, c'_2, c'_3 \rangle$. Moreover, $\langle c'_1, c'_2 - c'_1, c'_3 - c'_1 \rangle = \langle c'_1, c'_2, c'_3 \rangle$. Finally, if we recursively subtract from g any polynomial in g belonging to $\langle c'_1, c'_2 - c'_1, c'_3 - c'_1 \rangle$ till the only monomials in g are 1 and r, we get the same result as the preceding mapping. The polynomials $c'_1, c'_2 - c'_1, c'_3 - c'_1$ constitute what is called a *Gröbner basis* [GP02, Definition 1.6.1] of the ideal $\langle c'_1, c'_2, c'_3 \rangle$.

Gröbner bases are used in Computational Algebraic Geometry in order to compute a canonic representative of the remainder of the division of one polynomial by several polynomials generating a given ideal I. This canonic representative belongs to the quotient algebra of the ring of polynomials by the ideal I. The Gröbner basis for this system provides a set of polynomials that define uniquely the algebraic relationships between variables for the solutions of the system.

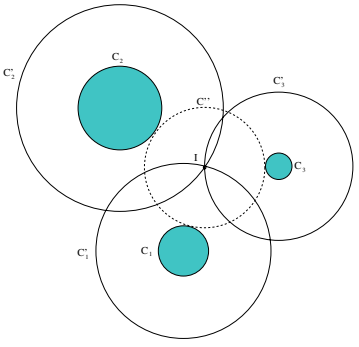

Fig. 13. The additively weighted Voronoi vertex as the common intersection of three expanding circles

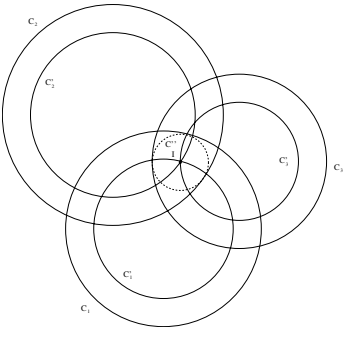

Fig. 14. The additively weighted Voronoi vertex as the common intersection of three shrinking circles

The initial (largest with respect to some monomial order [CLO98]) monomials of each one of the polynomials of the Gröbner basis form an ideal. The monomials that do not pertain to this ideal form a basis for the representatives of the equivalence class of the remainders of the division of a polynomial by the polynomials of the system in the quotient algebra. These monomials are called standard monomials. For the above Gröbner basis, the standard monomials are 1 and r. The size of this basis equals the *dimension* [GP02, see definition on page 414] of the quotient algebra and the number of solutions of the system counted with their multiplicity [Lan02]. In the case of the conflict locator for the additively weighted Voronoi diagram, there are two solutions.

The polynomial $g = (x_4 - x)^2 + (y_4 - y)^2 - (r + r_4)^2$ expresses the relative position of C_4 with respect to C''. Indeed C'' is tangent to C_4 if, and only if, the Euclidean distance between the centres of C'' and of C_4 (i.e., (x, y) and p_4) equals the sum of the radii r and r_4, i.e. $(x_4 - x)^2 + (y_4 - y)^2 - (r + r_4)^2 = 0$. The open balls bounded by C'' and C_4 intersect if, and only if, the Euclidean distance between the centres of C'' and of C_4 is smaller than the sum of the radii r and r_4, i.e. $(x_4 - x)^2 + (y_4 - y)^2 - (r + r_4)^2 < 0$. The circles C'' and C_4 are disjoint if,

and only if, the Euclidean distance between the centres of C'' and of C_4 is greater than the sum of the radii r and r_4, i.e. $(x_4 - x)^2 + (y_4 - y)^2 - (r + r_4)^2 > 0$. We considered the operation of multiplication of polynomials by the polynomial g. This *multiplication operator* is a linear mapping. The operation of this mapping on the canonic representative of the reminder of the division of a polynomial by c'_1, c'_2 and c'_3 is also a linear mapping that can be expressed by a matrix since the quotient algebra has a finite dimension.

First, we compute the matrix $M_g = \begin{pmatrix} m_{00} & m_{01} \\ m_{10} & m_{11} \end{pmatrix}$ of the following multiplication operator on the quotient algebra:
$m_g : [f] \longrightarrow [gf]$.

The eigenvalues of M_g are the values of g taken on X (see Theorem 4.5, page 54 in [CLO98]). The eigenvalues of M_g are the solutions of $det\,(M_g - \lambda I) = 0$, where I denotes the 2×2 identity matrix, i.e. the roots of

$$\lambda^2 - \lambda\,(m_{00} + m_{11}) + (m_{00}m_{11}) - (m_{01}m_{10}) = 0 \tag{4.1}$$

The values certifying the presence of Voronoi vertices in the list output by the Delaunay graph conflict locator are the signs of the values taken by g, and they are determined by the sign of the roots of Equation 4.1 (which are the eigenvalues of M_g). If there is only one eigenvalue and it is 0 then the fourth circle is tangent to the circle externally tangent to the first three circles. The sign of Δ (where $\Delta = (m_{00} + m_{11})^2 - 4\,(m_{00}m_{01} - m_{01}m_{10})$) cannot be negative when the first three sites of the input correspond to a Delaunay triangle, because this would be equivalent to the fact there would be no triangle with vertices C_1, C_2 and C_3 in the old Delaunay graph (because of the absence of real Voronoi vertex, see Figure 15). Thus, if $sign\,(\Delta)$ is negative that means we have one circle contained in another circle, and then we just need to link them by a Delaunay edge. Otherwise, $sign\,(\Delta)$ is 0 or positive, and we have to evaluate the sign of the roots of the quadratic equation.

When there is only one double root of Equation 4.1 then we have the following two possibilities. Either the value of the root of Equation 4.1 is positive or 0

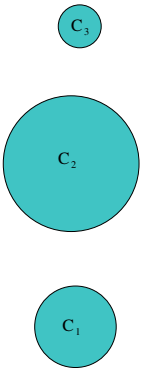

Fig. 15. There is no such triangle in the old Delaunay graph because of the absence of a real Voronoi vertex

and the triangle will exist in the new Delaunay graph, or the value of the root of Equation 4.1 is negative and the triangle will not exist in the new Delaunay graph (see Figure 12). When there are two real roots of Equation 4.1, we have two triangles to consider (see Figure 16). The triangles that correspond to the roots with a negative value will disappear in the new Delaunay graph (see Figure 16).

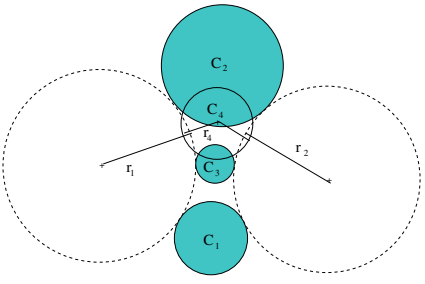

Fig. 16. Two triangles can possibly disappear simultaneously by the addition of a single weighted point

There is not much interest in showing the elements of the matrix of the multiplication operator here, but the Macaulay 2 [GS] code is presented in Appendix 1. The exact algebraic computation of the Delaunay graph conflict locator we have presented in the previous paragraph is not generalisable to the other proper conics or higher degree algebraic curves. Indeed, the size of the multiplication operator matrix is greater than 4 for the other proper conics and for higher degree algebraic curves, and an algebraic equation of degree 5 or more is not necessarily solvable by radicals (see [BB96, Theorem 8.4.8]). Even if we can obtain the matrix of the multiplication operator symbolically, we will need numerical methods for computing the eigenvalues of that matrix, which give the answer to the Delaunay graph conflict locator.

We will now present the Delaunay graph conflict locator for circles, emphasising the changes with respect to the Delaunay graph of additively weighted points presented in this subsection.

4.3 The Delaunay Graph Conflict Locator for Circles

Let $\mathcal{C} = \{C_1, ..., C_N\}$ be the set of generators or sites, with all the C_i being circles in $\mathbb{R}^2$. Let p_i be the centre of C_i and r_i be the radius of C_i.

The definitions of bisector, influence zone, Voronoi region and Voronoi diagram presented in Chapter 2 generalise to the case where the set of sites $\mathcal{S}$ is a set of circles $\mathcal{C}$, and the distance $d(M, C_i)$ between a point M and a site C_i is the Euclidean distance between M and the closest point on C_i from M, i.e. $d(M, C_i) = |\delta(M, p_i) - r_i|$, where δ is the Euclidean distance between points. Observe that assuming C_i is centred on p_i and $r_i = w_i$ for $i = 1, .., N$, this distance

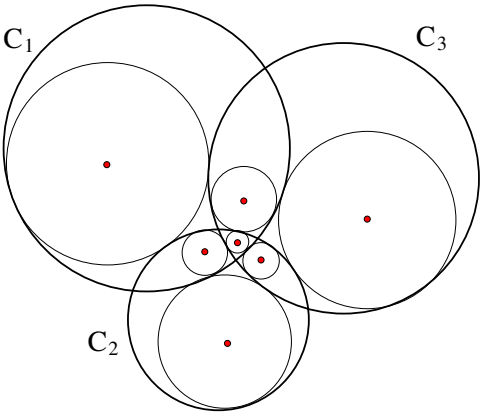

Fig. 17. Seven Apollonius circles centres that are true Voronoi vertices (first case)

is the absolute value of the additive distance used in the previous subsection. The Voronoi region of C_i with respect to the set $\mathcal{C}$ is thus defined by:

$$\mathcal{V}(C_i, \mathcal{C}) = \left\{ M \in \mathbb{R}^2 | \forall j \neq i : |\delta(M, p_i) - r_i| < |\delta(M, p_j) - r_j| \right\}.$$

The Voronoi diagram of $\mathcal{C}$ is defined by: $V(\mathcal{C}) = \bigcup_{C_i \in \mathcal{C}} \partial V(C_i, \mathcal{C})$.

In the previous subsection, we observed that two Apollonius circles centres are true Voronoi vertices of the additively weighted Voronoi diagram (the circles that are either externally or internally tangent to three given circles). When the sites are circles, up to seven of the eight Apollonius circles may be relevant to the Delaunay graph conflict locator (see Figure 17).

We consider the maintenance of the Delaunay graph of circles in an incremental way: we check first the validity of all the old triangles of the Delaunay graph whose vertices are a given triple of circles with respect to a given newly inserted circle. When old triangles are checked, four circles C_1, C_2, C_3 and C_4 are given: the first three are supposed to define one or more triangles in the Delaunay graph, and the last one is the newly inserted circle. Let (x_i, y_i) be the coordinates of p_i for $i = 1, 2, 3, 4$. There are two possible outcomes to the above test of validity. Either the triangles are valid with respect to the newly inserted weighted point and the triangles remain in the new Delaunay graph, or there is at least one triangle that is not valid with respect to the newly inserted weighted point and these triangles will not be present in the Delaunay graph any longer. We also need to check the validity of new triangles $C_1C_2C_3$ with respect to a circle C_4, where $C_1C_2C_4$ is an old Delaunay triangle and C_3 is the newly inserted circle. There are two possible outcomes to this test of validity. Either the triangles formed with an old Delaunay edge C_1C_2 and the newly inserted weighted point C_3 are valid with respect to any circle C_4, where $C_1C_2C_4$ is an old Delaunay triangle, and the triangles will appear in the new Delaunay graph, or there is at least one triangle that is not valid and these triangles will not be added in the Delaunay graph. In both cases, we check the validity of a triangle $C_1C_2C_3$ with respect to a circle C_4.

The Apollonius circles of C_1, C_2 and C_3 can be obtained algebraically by computing the common intersection of the three circles C_1', C_2' and C_3' (see Figure 13) expanding or shrinking from the three first circles C_1, C_2 and C_3 all with the same absolute value of the rate. The common unsigned expansion of the first three circles is denoted by r. The coordinates of the intersection I of C_1', C_2' and C_3' are denoted (x, y). The circle C'' centred on (x, y) and of radius r is tangent to the first three circles.

Thus, the Apollonius circles are the solutions of one of the eight following systems (I) of three quadratic equations in three unknowns x, y, r:

$$\begin{cases} (x - x_1)^2 + (y - y_1)^2 - (r_1 \pm r)^2 = 0 \\ (x - x_2)^2 + (y - y_2)^2 - (r_2 \pm r)^2 = 0 \\ (x - x_3)^2 + (y - y_3)^2 - (r_3 \pm r)^2 = 0 \end{cases}.$$

By replacing r by $-r$ in one of the preceding systems of equations, we still get another one of the preceding systems of equations. Thus, let us suppose r is the signed expansion of C_1. Then, we can reformulate the preceding systems of equations as the following systems (II) of equations:

$$\begin{cases} (x - x_1)^2 + (y - y_1)^2 - (r_1 + r)^2 = 0 \\ (x - x_2)^2 + (y - y_2)^2 - (r_2 \pm r)^2 = 0 \\ (x - x_3)^2 + (y - y_3)^2 - (r_3 \pm r)^2 = 0 \end{cases}$$

Now let us consider for each system (II) the set X of solutions of the system (II) of equations in K^3, where K is an algebraically closed field.

Subtracting one of the equations from the remaining two results in a system of 2 linear equations, from which x and y may be expressed as linear functions of r. Substitution in the first equation then leads to a quadratic equation in r. This means that the unknown quantities x, y, r can be expressed with quadratic radicals as functions of the given centres and radii for each one of the systems of equations above.

As before, though the simplest thing to do now would be to compute the two Voronoi vertices and use their computed coordinates and corresponding signed expansion in the computation of the values certifying the output of the Delaunay graph conflict locator, it is not desirable because this method would not be generalisable to conics or higher degree curves.

For the Delaunay graph of additively weighted points, the true Voronoi vertices are the solutions of one system of algebraic equations. Unlike the previous case, for the Delaunay graph of circles, the true Voronoi vertices are not all the solutions of one system of algebraic equations, but a subset of the solutions of four systems of algebraic equations. The solutions of the algebraic equations are the Apollonius circles, whose centres are generalised Voronoi vertices (a concept that was introduced in [Anton04]). We thus need to determine which Apollonius circles centres are potentially true Voronoi vertices (only the real Apollonius circles centres can be true Voronoi vertices).

There are four possible determinations of the true Voronoi vertices from Apollonius circles centres of C_1, C_2 and C_3:

First case. If C_1, C_2 and C_3 mutually intersect, then the real circles among the seven Apollonius circles that are not internally tangent to each of C_1, C_2 and C_3 correspond to true Voronoi vertices (their centres are true Voronoi vertices, see Figure 17), and reciprocally.

Second case. If one circle (say C_1) intersects the two others (C_2 and C_3) which do not intersect, then only the real Apollonius circles that are either externally tangent to each of C_1, C_2 and C_3, or internally tangent to C_1 and externally tangent to C_2 and C_3 correspond to true Voronoi vertices (their centres are true Voronoi vertices, see Figure 18).

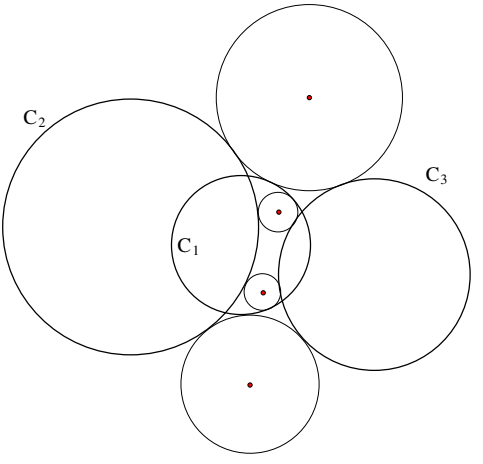

Fig. 18. Four Apollonius circles centres that are true Voronoi vertices (second case)

Third case. If two circles (say C_1 and C_2) intersect the interior of the third one (C_3) and at least one of them (say C_1) is contained in the interior of C_3, then only the real Apollonius circles that are externally tangent to C_1 and C_2 and internally tangent to C_3 correspond to true Voronoi vertices (their centres are true Voronoi vertices, see Figure 19).

Fourth case. Otherwise (if none of the three situations above apply), only the real Apollonius circles that are externally tangent to C_1, C_2 and C_3 correspond to true Voronoi vertices (their centres are true Voronoi vertices, see Figure 20).

When the old Delaunay triangles are checked, the case where one circle (say C_1) lies in the interior of a second circle (say C_2), which lies in the interior of the third circle (C_3), or only one circle (say C_1) lies within the interior of one of the other ones (say C_2) cannot happen because then, there would be no Voronoi vertices and the triangle $C_1C_2C_3$ would not exist in the Delaunay graph. If we check new triangles, we can check if the situation described just above happens by computing the sign of the determinant of the multiplication matrix for the fourth case.

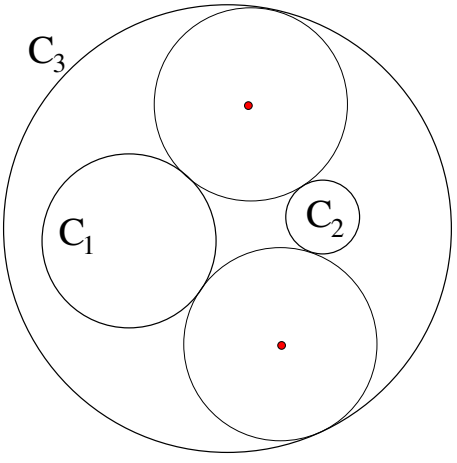

Fig. 19. Two Apollonius circles centres that are true Voronoi vertices (third case)

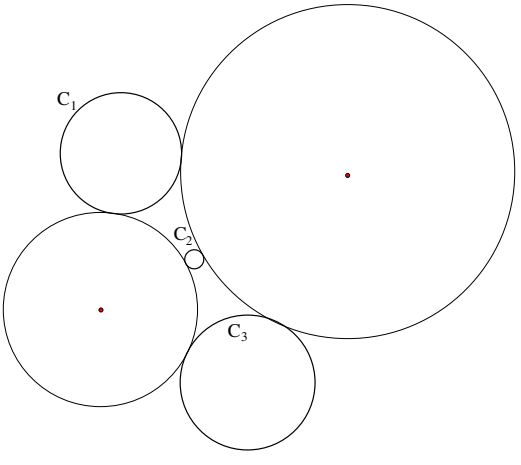

Fig. 20. Two Apollonius circles centres are true Voronoi vertices (fourth case)

Now that we have seen the different cases of true Voronoi vertices, we will see how we can test in which case we are and which solutions of the systems of equations (II) described above correspond to true Voronoi vertices.

First case. C_1, C_2 and C_3 mutually intersect if, and only if, $d(p_1, p_2) - r_1 - r_2 \leq 0$ and $d(p_1, p_3) - r_1 - r_3 \leq 0$ and $d(p_2, p_3) - r_2 - r_3 \leq 0$. The computation of this test can be done exactly, since the only variables that are not input to the Delaunay graph conflict locator are the distances, and these distances are expressed by radicals. Indeed, we need to test the sign of the difference of a radical and a number which do not depend on intermediary computations. The true Voronoi vertices are the real solutions of all the systems of equations (II) such that $r > 0$.

Second case. C_1 intersects C_2 and C_3, and C_2 and C_3 have no point of intersection if, and only if, $d(p_1, p_2) - r_1 - r_2 \leq 0$ and $d(p_1, p_3) - r_1 - r_3 \leq 0$ and $d(p_2, p_3) - r_2 - r_3 > 0$. The computation of this test can be done exactly for the same reasons as the previous case. The true Voronoi vertices are the real solutions of the system of equations:

$$\begin{cases} (x - x_1)^2 + (y - y_1)^2 - (r_1 \pm r)^2 = 0 \\ (x - x_2)^2 + (y - y_2)^2 - (r_2 - r)^2 = 0 \\ (x - x_3)^2 + (y - y_3)^2 - (r_3 - r)^2 = 0 \end{cases}$$

with $r < 0$.

Third case. C_1 lies in the interior of C_3 and C_2 intersects the interior of C_3 if, and only if, $d(p_1, p_3) + r_1 - r_3 < 0$ and $d(p_2, p_3) - r_2 - r_3 < 0$ and $(x_1 - x_3)^2 + (y_1 - y_3)^2 - r_3^2 < 0$. The computation of this test can be done exactly for the same reasons as the previous case. The true Voronoi vertices are the real solutions of the system of equations:

$$\begin{cases} (x - x_1)^2 + (y - y_1)^2 - (r_1 + r)^2 = 0 \\ (x - x_2)^2 + (y - y_2)^2 - (r_2 + r)^2 = 0 \\ (x - x_3)^2 + (y - y_3)^2 - (r_3 - r)^2 = 0 \end{cases}$$

such that $r > 0$.

Fourth case. this is the case if all the previous three tests failed. The true Voronoi vertices are the real solutions of the system of equations:

$$\begin{cases} (x - x_1)^2 + (y - y_1)^2 - (r_1 + r)^2 = 0 \\ (x - x_2)^2 + (y - y_2)^2 - (r_2 + r)^2 = 0 \\ (x - x_3)^2 + (y - y_3)^2 - (r_3 + r)^2 = 0 \end{cases}$$

with $r > 0$.

As before, we used the same algebraic machinery to compute the values of polynomials that are taken by the true Voronoi vertices without solving any intermediate system of equations. We computed the Gröbner basis of the ideal of X for each one of the systems (II) encountered. Each one of these Gröbner bases consists of the earlier mentioned quadratic equation in r and linear equations in x, y and r.

For the Delaunay graph of additively weighted points, we observed that evaluating the signs of a single polynomial ($g = (x_4 - x)^2 + (y_4 - y)^2 - (r + r_4)^2$) taken on the real points of X was enough to provide the values certifying the presence of Voronoi vertices in the list output by the conflict locator. As before, we can check for the existence of real solutions by evaluating the sign of the discriminant of the characteristic polynomial. We will suppose the real solutions to the systems (II) have been tested. Unlike in the previous case, here we need to evaluate the signs taken by both g and r on each one of the points of X. Indeed, we need not only to check the relative position of C_4 with respect to the Apollonius circles, but we need for each Apollonius circle, to check the relative position of C_4 with respect to that Apollonius circle, and to check whether that Apollonius circle corresponds to a true Voronoi vertex.

As before, we considered the operation of multiplication of polynomials by the polynomial g, whose sign expresses the relative position of C_4 with respect to C''. We also considered the operation of multiplication of polynomials by the polynomial r, whose sign allows one to check whether the solutions correspond to true Voronoi vertices. These operations are linear mappings. The operations of these mappings on the canonic representative of the remainder of the Euclidean division of a polynomial by the three polynomials of the system are also linear mappings that can be expressed by a matrix.

We need to be able to associate the signs of the values of g with the signs of the values of r taken on the (real) solutions of each system (II). For a given system (II), let M_g and M_r be the matrices of the result of the multiplication by g and by r respectively on the canonic representative of the remainder of the division of a polynomial by the three polynomials of the system. Since these multiplication maps commute, it is possible to use the transformation matrix obtained during the computation of the Jordan form of one of these matrices to triangularise the other matrix by a simple multiplication of matrices [CLO98]. Indeed, the computation of the Jordan form for M_g gives the triangular matrix $P^{-1}M_gP$ of the Schur form of that matrix where P is a unitary matrix called the transformation matrix; and $P^{-1}M_rP$ is triangular. Finally, we can obtain the solutions by reading the diagonal entries in turn in each one of the Jordan forms of these matrices (the diagonal entries of the Jordan form of a matrix are its eigenvalues). The row number on each one of these matrices corresponds to the index of the solution. By evaluating the signs of the diagonal entries in the Jordan forms of M_g and of M_r on the same line, we associate the signs of the values of g with the signs of the values of r taken on the solutions of each system (II).

5 The Application to the Visualization of the Nucleation and Growth of Particles

The algorithm described in the previous section is applied in this section to the computation of the Johnson-Mehl tessellation, which is a special case of Voronoi diagram of circles. The dual graph of the Johnson-Mehl tessellation is

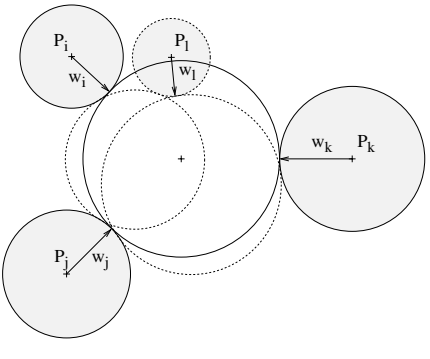

Fig. 21. The event that changes the topology

a triangulation. Now, we will examine the events that affect this triangulation (see Figure 21).

Proposition 9. *(The empty circumcircle criterion for the dual graph of the Johnson-Mehl tessellation): A triangle* $P_i \overset{\triangle}{P_j} P_k$ *exists in the triangulation if, and only if, the circle externally (respectively internally) tangent to the weight circles* $\mathcal{C}(P_i, w_i)$, $\mathcal{C}(P_j, w_j)$, *and* $\mathcal{C}(P_k, w_k)$, *does not intersect properly (non tangentially) any other circle* $\mathcal{C}(P_l, w_l)$, $l \notin \{i, j, k\}$.

Proof. If a fourth circle $\mathcal{C}(P_l, w_l)$ happens to be externally (respectively internally) tangent to the circle $\mathcal{C}_{t_{\{i,j,k\}}}$ that is externally (respectively internally) tangent to $\mathcal{C}(P_i, w_i)$, $\mathcal{C}(P_j, w_j)$, and $\mathcal{C}(P_k, w_k)$, then the vertex $v_{\{i,j,k\}}$ (intersection of $\mathcal{B}_{ij}$, $\mathcal{B}_{ik}$, and $\mathcal{B}_{jk}$) is 4-valent, and the triangle exists in the Delaunay graph.

Otherwise, if the intersection of $\mathcal{C}(P_l, w_l)$ and $\mathcal{C}_{t_{\{ijk\}}}$ was constituted by two different points, then $\mathcal{C}_{t_{\{i,j,l\}}}$ and $\mathcal{C}_{t_{\{j,k,l\}}}$ would be externally (respectively internally) tangent to $\mathcal{C}(P_i, w_i)$, $\mathcal{C}(P_j, w_j)$, and $\mathcal{C}(P_l, w_l)$; and $\mathcal{C}(P_j, w_j)$, $\mathcal{C}(P_k, w_k)$, and $\mathcal{C}(P_l, w_l)$ respectively. Then we would have the triangles $P_i \overset{\triangle}{P_j} P_k$, $P_i \overset{\triangle}{P_j} P_l$, and $P_j \overset{\triangle}{P_k} P_l$, which would contradict the fact that the dual graph of the Johnson-Mehl tessellation is a triangulation (see Figure 22). □

We should therefore make a triangle switch: replace $P_i \overset{\triangle}{P_j} P_k$ and $P_i \overset{\triangle}{P_k} P_l$ by $P_i \overset{\triangle}{P_j} P_l$ and $P_j \overset{\triangle}{P_k} P_l$. Proposition 1 implies that the triangulation mentioned above obeys the Delaunay triangulation "empty circumcircle criterion". This follows the algorithm of Guibas and Stolfi [GS85] for the ordinary Voronoi diagram, extending it to this case of a generalized Dirichlet tessellation. This proposition is the basis of the incremental algorithm that we implemented for the dynamic construction and maintenance of additively weighted Voronoi diagrams. When a new point is added, we locate the triangle T in which it lies, then we connect this new point to the triangulation by replacing T by three new triangles whose vertices are the vertices of T and the new point. Then we check every circle externally respectively internally tangent to the weight circles of the points of every new triangle. If a triangle switch (see Figure 22) has to be performed (see end of the Proof of Proposition 9), we perform the same check for all the externally respectively internally tangent circles corresponding to the triangles generated by the triangle switch (see Figure 2 where the triangle switch is shown: replacing $P_i \overset{\triangle}{P_j} P_k$ and $P_i \overset{\triangle}{P_k} P_l$ by $P_i \overset{\triangle}{P_j} P_l$ and $P_j \overset{\triangle}{P_k} P_l$).

When an existing point is deleted, we locate its nearest neighbour, then we transfer all its neighbours to the nearest neighbour and we remove it and its topological relationships from the triangulation. Then we check every circle externally respectively internally tangent to the weight circles of the points of every modified triangle. If a triangle switch has to be performed (see end of the Proof of Proposition 9), we perform the same check for all the externally respectively internally tangent circles corresponding to the triangles generated by the triangle switch. This is the basis of the incremental algorithm [AMG98a], that we

implemented for the dynamic construction and maintenance of Johnson-Mehl tessellation.

Our algorithm proceeds in a fashion analogous to the algorithm of Devillers, Meiser, and Teillaud [DMT90] for the dynamic Delaunay triangulation based on the Delaunay tree. They proved using the Delaunay tree that each insertion and point location has an expected running time of $O(\log n)$, and each deletion has an expected running time of $O(\log \log n)$. Our algorithm has an efficiency of $O(\log n)$.

5.1 The Johnson-Mehl Tessellation

The algorithm for the construction of the Voronoi diagram of circles has been adapted in order to get the incremental algorithm for the construction and maintenance of the Johnson-Mehl model. After each arrival of a new nucleus, the Johnson-Mehl tessellation changes, and we recompute it as follows. The new nucleus is inserted in the Johnson-Mehl tessellation (a new Voronoi region appears), and the neighbouring Voronoi cells are changed. The size of the spheres is then increased by the growth corresponding to the time interval between the previous insertion and this one $(t_i - t_j)$. Consequently, the spheres will be increased for this time interval (see Figures 22 and 23). This type of spatial growth uses a Poisson point process [OBSC01], and we will now introduce two different cases of radial speed for spatial growth processes.

Time homogeneous Poisson point process. The uniform radial growth of the nuclei and appearance of their Voronoi regions at two different times is shown in Figures 22 and 23. On Figures 22 and 23, we can see the growth of the spheres between two time units. We notice that the Voronoi regions are changed only when a new particle appears.

We assume [Stoya98] that the radial growth speed is the same for all the spheres, and the growth of the spheres in the portion of contact is stopped (see Figures 22 and 23). In the early stages of growth and nucleations spheres do not overlap, but after a certain time a sphere may touch another sphere [OBSC01].

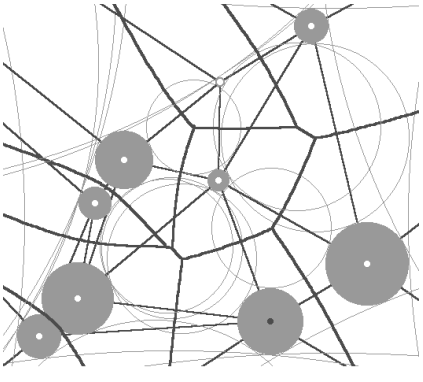

Fig. 22. The growth of particles at $t = 93$

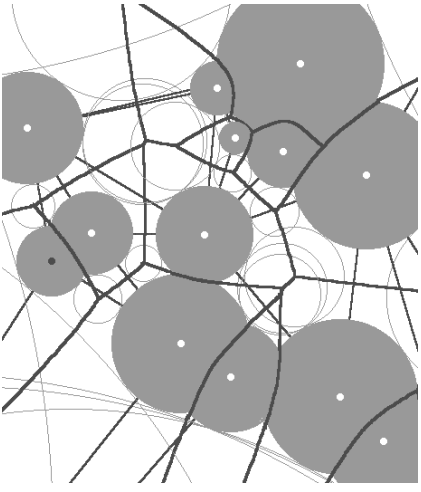

Fig. 23. The growth of particles at $t = 163$

Time inhomogeneous Poisson point process. The Johnson-Mehl model has been generalized [OBSC01] in three different ways: changing the spatial location process for the generators (nuclei), changing the birth rate of the generators, or both. The most extensively studied generalization is the generalization corresponding to the change of the nuclei birth rate as a function of time without changing the spatial location process (the homogeneous Poisson point process). This generalization is known as the time inhomogeneous Johnson-Mehl model. The algorithm for the construction and maintenance of the Johnson-Mehl model is also applied in the case of a time inhomogeneous Poisson point process. In that case, all the nuclei grow at the same radial speed for each time interval and therefore, as long as a new nucleus does not arrive, the difference between the weights of neighbouring nuclei is constant, and the Johnson-Mehl tessellation does not change.

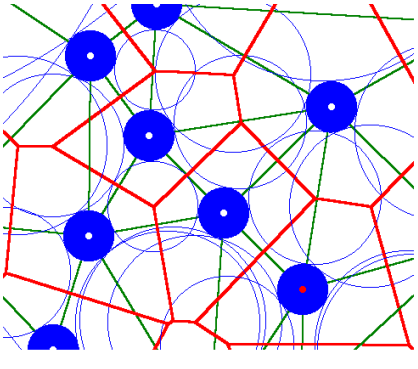

Fig. 24. The Voronoi growth model at $t = 31$

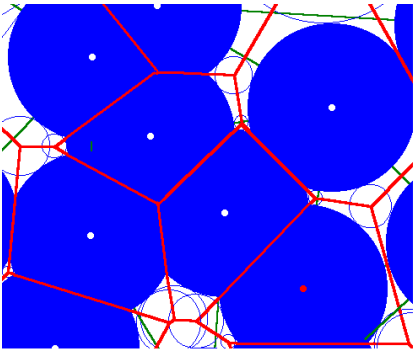

Fig. 25. The Voronoi growth model at $t = 96$

5.2 The Voronoi Growth Model

The Additively Voronoi diagram reduces to the ordinary Voronoi diagram when all the w_i are equal to some constant. In that type of particle growth, nucleation occurs simultaneously. In Figure 24 we can see the simultaneous appearance of the nuclei that are all of the same size. Figure 25 shows the growth of these particles after 65 time units (shown in increased weights). We notice that the tessellation has not changed.

Thus, for the nucleation sites that are appearing simultaneously we have a non-Poisson point process [Stoya98] and we can apply our algorithm that reduces the Johnson-Mehl model to the Voronoi growth model.

6 Conclusions

We have provided a predicate for the incremental construction of the Delaunay graph and the Voronoi diagram of circles that amounts to computing the sign of the eigenvalues of a two by two matrix. Unlike other independent research, our work proposes a single predicate that can compute the Delaunay graph even in the case of one circle being entirely in another circle or intersecting circles. We have also provided an application of the Voronoi diagram of circles to the modelling and the visualisation of the growth of crystal aggregates. We have been also working on the Delaunay graph of conics and of semi-algebraic sets (see [Anton04]), and future work include the Delaunay graph and Voronoi diagram of quadrics and its applications.

References

[AB86] Ash, P.F., Bolker, F.D.: Generalized Dirichlet Tessellations. Geometria Dedicata 20, 209–243 (1986)

[ABMY02] Anton, F., Boissonnat, J.-D., Mioc, D., Yvinec, M.: An exact predicate for the optimal construction of the Additively Weighted Voronoi diagram. In: Proceedings of the European Workshop on Computational Geometry 2002, Warsaw, Poland (2002)

[AK00] Aurenhammer, F., Klein, R.: Voronoi diagrams. In: Handbook of computational geometry, pp. 201–290. North-Holland, Amsterdam (2000)

[AKM02] Anton, F., Kirkpatrick, D., Mioc, D.: An exact algebraic predicate for the maintenance of the topology of the additively weighted voronoi diagram. In: The Fourteenth Canadian Conference on Computational Geometry, Lethbridge, Alberta, Canada, pp. 72–76 (2002)

[AM95] Anishchik, S.V., Medvedev, N.N.: Three-dimensional Apollonian packing as a model for dense granular systems ll. Phys. Rev. Lett. 75(23), 4314–4317 (1995)

[AMG98a] Anton, F., Mioc, D., Gold, C.M.: Dynamic Additively Weighted Voronoi Diagrams Made Easy. In: Proceedings of the 10^{th} Canadian Conference on Computational Geometry (CCCG 1998), Montréal, Canada (1998)

[AMG98b] Anton, F., Mioc, D., Gold, C.M.: An algorithm for the dynamic construction and maintenance of Additively Weighted Voronoi diagrams. In: Proceedings of the 14^{th} European Workshop on Computational Geometry (CG 1998), Barcelona, Spain, pp. 117–119 (1998)

[Anton04] Anton, F.: Voronoi diagrams of semi-algebraic sets, Ph.D. thesis, The University of British Columbia, Vancouver, British Columbia, Canada (2004)

[Auren87] Aurenhammer, F.: Power diagrams: properties, algorithms and applications. SIAM J. Comput. 16(1), 78–96 (1987)

[Auren88] Aurenhammer, F.: Voronoi diagrams - A survey, Institute for Information Processing, Technical University of Graz, Report 263 (1988)

[BB96] Beachy, J.A., Blair, W.D.: Abstract Algebra. Waveland Press Inc. (1996)

[BCSS98] Blum, L., Cucker, F., Shub, M., Smale, S.: Complexity and real computation. Springer, New York (1998) (with a foreword by R.M. Karp)

[Berge79] Berger, M.: Géométrie. espaces euclidiens, triangles, cercles et sphères, CEDIC/FERNAND NATHAN, Paris, vol. 2 (1979)

[Boots73] Boots, B.N.: Some models of random subdivision of space. Geografiska Annaler 55B, 34–48 (1973)

[CLO98] Cox, D., Little, J., O'Shea, D.: Using algebraic geometry. Springer, New York (1998)

[CPX02] Chen, Z., Papadopoulou, E., Xu, J.: Robust algorithm for k-gon voronoi diagram construction. In: Abstracts for the Fourteenth Canadian Conference on Computational Geometry CCCG 2002, Lethbridge, Alberta, Canada, August 2002, pp. 77–81. University of Lethbridge (2002)

[Des03] Deschamps, A.: Analytical Techniques for Aluminium Alloys. In: Handbook of Aluminum. Alloy Production and Materials manufacturing, vol. 2, pp. 155–192. Marcel Dekker, Inc., New York (2003)

[DMT90] Devillers, O., Meiser, S., Teillaud, M.: Fully Dynamic Delaunay Triangulation in Logarithmic Expected Time per Operation, Rapport INRIA 1349, INRIA, BP93, 06902 Sophia-Antipolis cedex, France (1990)

[EK06] Emiris, I.Z., Karavelas, M.I.: The predicates of the Apollonius diagram: algorithmic analysis and implementation. Comput. Geom. 33(1-2), 18–57 (2006)

[GP02] Greuel, G.-M., Pfister, G.: A Singular introduction to commutative algebra. In: Bachmann, O., Lossen, C., Schönemann, H. (eds.), With 1 CD-ROM (Windows, Macintosh, and UNIX). Springer, Berlin (2002)

[GS] Grayson, D.R., Stillman, M.E.: Macaulay 2, a software system for research in algebraic geometry, `http://www.math.uiuc.edu/Macaulay2/`

[GS85] Guibas, L., Stolfi, J.: Primitives for the Manipulation of General Subdivisions and the Computation of Voronoi Diagrams. ACM Transactions on Graphics 4(2), 74–123 (1985)

[Horal79] Horalek, V.: The Johnson-Mehl tessellation with time dependent nucleation intensity in view of basic 3-D tessellations. Mathematical research 51, 111–116 (1979)

[JM39] Johnson, W.A., Mehl, F.R.: Reaction kinetics in processes of nucleation and growth. Transactions of the American Institute of Mining, Metallurgical and Petroleum Engineers 135, 416–456 (1939)

[KE02] Karavelas, M.I., Emiris, I.Z.: Predicates for the Planar Additively Weighted Voronoi Diagram. ECG Technical Report ECG-TR-122201-01, INRIA (2002)

[KE03] Karavelas, M.I., Emiris, I.Z.: Root comparison techniques applied to computing the additively weighted Voronoi diagram. In: Proceedings of the Fourteenth Annual ACM-SIAM Symposium on Discrete Algorithms, Baltimore, MD, pp. 320–329. ACM, New York (2003)

[KKS00] Kim, D.-S., Kim, D.-U., Sugihara, K.: Voronoi diagram of a circle set constructed from Voronoi diagram of a point set. In: Lee, D.T., Teng, S.-H. (eds.) ISAAC 2000. LNCS, vol. 1969, pp. 432–443. Springer, Heidelberg (2000)

[KKS01a] Kim, D.-S., Kim, D., Sugihara, K.: Voronoi diagram of a circle set from Voronoi diagram of a point set. I. Topology. Comput. Aided Geom. Design 18(6), 541–562 (2001)

[KKS01b] Kim, D.-S., Kim, D., Sugihara, K.: Voronoi diagram of a circle set from Voronoi diagram of a point set. II. Geometry. Comput. Aided Geom. Design 18(6), 563–585 (2001)

[Kle89] Klein, R.: Concrete and abstract Voronoï diagrams. Springer, Berlin (1989)

[Kol37] Kolmogorov, A.N.: A statistical theory for the recrystallization of metals. Akad. nauk SSSR, Izv., Ser. Matem. 1(3), 355–359 (1937)

[Lan02] Lang, S.: Algebra, 3rd edn. Graduate Texts in Mathematics, vol. 211. Springer, New York (2002)

[Med00] Medvedev, N.N.: Voronoi-Delaunay method for non-crystalline structures. SB Russian Academy of Science, Novosibirsk (2000)

[OBSC01] Okabe, A., Boots, B., Sugihara, K., Chiu, S.N.: Spatial Tessellations: Concepts and Applications of Voronoi Diagrams. John Wiley & Sons, Chichester (2001)

[Stoya98] Stoyan, D.: Random sets: Models and Statistics. International Statistical Review 66, 1–27 (1998)

[Vor07] Voronoï, G.F.: Nouvelles applications des paramètres continus à la théorie des formes quadratiques. premier mémoire. sur quelques propriétés des formes quadratiques positives parfaites. Journal für die reine und angewandte Mathematik 133, 97–178 (1907)

[Vor08] Voronoï, G.F.: Nouvelles applications des paramètres continus à la théorie des formes quadratiques. deuxième mémoire. recherches sur les parallélоèdres primitifs. première partie. partition uniforme de l'espace analytique à n dimensions à l'aide des translations d'un même polyèdre convexe. Journal für die reine und angewandte Mathematik 134, 198–287 (1908)

[Vor10] Voronoï, G.F.: Nouvelles applications des paramètres continus à la théorie des formes quadratiques. deuxième mémoire. recherches sur les paralléloèdres primitifs. seconde partie. domaines de formes quadratiques correspondant aux différents types de paralléloèdres primitifs. Journal für die reine und angewandte Mathematik 136, 67–181 (1910)

Appendix 1

The Macaulay 2 program for the exact Delaunay graph conflict locator for circles

```
gbTrace 4
dim FractionField  :=   F  ->  0
P  =  frac(QQ[a,b,c,d,e,f,g,h,i,j,k,l])
R = P[x,y,t]
cercle1 = (x-a)^2+(y-b)^2-(c+t)^2
cercle2 = (x-d)^2+(y-e)^2-(f+t)^2
cercle3 = (x-g)^2+(y-h)^2-(i+t)^2
emptycircle  =  ideal(cercle1,cercle2,cercle3)
ecgb  =  gb  emptycircle
print  ecgb
eckb  =  basis  cokernel  gens  ecgb
print  eckb
 kl  =  sort(flatten(entries(eckb)))
 kmind  =  splice {0..#kl - 1}
scan(kl,entry->print ring entry);
hashlist  =  pack(2,mingle(kl,kmind));
 feetmon  =  applyKeys(hashTable hashlist, key->toString(key));
compmat = f -> (htl=apply(kl,be->
hashTable(pack(2,mingle(apply(flatten(entries((coefficients((f*be)
%ecgb))#0)),
item  ->  feetmon#(toString(item))),flatten(entries((coefficients
((f*be)%ecgb))#1))))));
matrix(table(#kl,#kl,(i,j)->if  (htl#i)#?j  then  (htl#i)#j  else
0)));
matp2  =  compmat((x-j)^2+(y-k)^2-(t+l)^2);
m00  =  matp2_(0,0)
m01  =  matp2_(0,1)
m10  =  matp2_(1,0)
m11  =  matp2_(1,1)
cm00  =  coefficients m00
cm000  =  cm00#0
cm001  =  cm00#1
cm01  =  coefficients m01
cm010  =  cm01#0
cm011  =  cm01#1
cm10  =  coefficients m10
cm100  =  cm10#0
cm101  =  cm10#1
cm11  =  coefficients m11
cm110  =  cm11#0
cm111  =  cm11#1
```